Superconductivity of divalent Chevrel phases at very high pressures

Y. S. Yao and R. P. Guertin
Physics Department, Tufts University, Medford, Massachusetts 02155

D. G. Hinks, J. Jorgensen, and D. W. Capone II
Materials Science Division, Argonne National Laboratory, Argonne, Illinois 60439
(Received 28 October 1987)

The electrical resistivity and the superconducting transition temperatures were examined for three representative divalent Chevrel phase systems, $SnMo_6S_8$, $EuMo_6S_8$, and $BaMo_6S_8$, as a function of hydrostatic pressure to 2 GPa and in quasihydrostatic pressures to 10 GPa. In all systems, T_c is depressed to 0 K for sufficiently large pressures. For the Sn- and Eu-based systems, both highly purified samples and samples with controlled oxygen content were used. In an oxygenated $SnMo_6S_8$ sample (less than 3% O_2 substituted for the S atoms) the pressure threshold and maximum T_c are 40% lower than in the pure sample, but for $P > 3.5$ GPa the T_c-P phase diagrams nearly coincide, with T_c reaching zero at an extrapolated pressure of about 12 GPa. In pure $EuMo_6S_8$, superconductivity appears only above a threshold pressure of about 1 GPa and is depressed to 0 K above 4.5 GPa. In an oxygenated sample the maximum T_c and the threshold pressure are depressed, and above about 3.5 GPa the T_c-P phase diagrams coincide, as in the Sn-based system, although T_c is then rapidly depressed to 0 K at about 4.5 GPa. In a highly purified $BaMo_6S_8$ sample superconductivity appears above about 2 GPa and is depressed to 0 K at extrapolated pressures above 12 GPa. A full transition to the zero-resistance superconducting state is observed in $BaMo_6S_8$. The data are discussed in terms of a model linking the rhombohedral-to-triclinic structural transition, the superconducting transition temperature, and the role of pressure in suppressing the structural transition.

INTRODUCTION

Interest in the Chevrel-phase superconducting systems has centered largely on the very high upper critical fields, H_{c2}, of several of the divalent systems such as $PbMo_6S_8$, and on the interplay of superconductivity and magnetism which occurs when magnetic ions are substituted on the metallic cation site.[1] Until the recent discovery of high-T_c ceramic-oxide superconductivity, Chevrel phases showed the largest upper critical fields. A dramatic illustration of the effect of magnetic ions in the high-field properties of a Chevrel phase superconductor was the observation of Meul *et al.*[2] of magnetic-field-induced superconductivity. Finally, the exchange interaction between localized magnetic moments and conduction electrons in Chevrel phases is weak, and this allows superconductivity to exist simultaneously with several types of magnetic order on the magnetic sublattices.

Few classes of superconducting materials have shown the extreme sensitivity to the application of pressure as the Chevrel phase systems.[3] Consequently, pressure has proven to be an important controllable parameter in the study of the Chevrel phases. For those systems which superconduct at ambient pressure, the application of additional pressure rather rapidly depresses the superconducting properties. For example, $dT_c/dP = -0.02$ K/GPa for pure $SnMo_6S_8$, more than four times that of elemental Sn.[3] For $EuMo_6S_8$ (Ref. 4) and $BaMo_6S_8$ (Ref. 5), both of which show semiconducting properties at ambient pressure, externally applied pressure first causes a sudden onset of superconductivity with fairly high transition temperatures, and then T_c decreases with further pressure.[6] However, in the case of the Ba-based system, the presence of bulk superconductivity at high pressure has been called into question.[7] X-ray diffraction studies show that for both $EuMo_6S_8$ and $BaMo_6S_8$ a structural transition takes place separating the high-temperature rhombohedral phase $R\bar{3}$ (which is favorable for superconductivity in divalent Chevrel phases) from a lower temperature triclinic phase $P\bar{1}$ (which is not superconducting).[4,8] In the triclinic phase a gap in the excitation spectrum presumably opens at the Fermi surface, which is consistent with the semiconducting behavior of these systems below the structural transition. This transition takes place around 100 K in $EuMo_6S_8$ (Ref. 4) and between 120 K and 180 K for $BaMo_6S_8$, depending on sample preparation.[8]

Previous pressure studies in Chevrel phase systems can be dated from the initial work of Shelton.[9] Extensive quasihydrostatic pressure measurements were more recently performed by Janawadkar *et al.*,[10] who studied the relationship between the structural instability and superconductivity in pressures to 7 GPa for $EuMo_6S_8$. Recently, Jorgensen and Hinks,[11] using high-resolution powder neutron diffraction data, revealed that even the much-studied systems $PbMo_6S_8$ and $SnMo_6S_8$ exhibit a small structural distortion from the rhombohedral phase below about 110 K and 130 K, respectively. Further

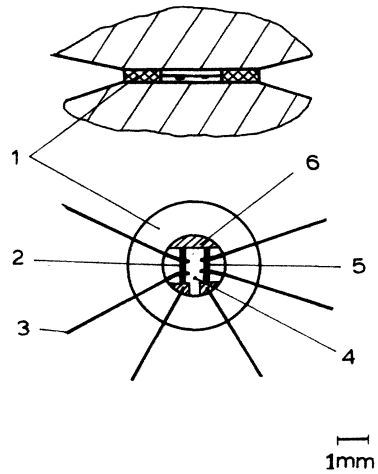

FIG. 1. Detail of the quasihydrostatic pressure cell. 1 denotes the pyrophilite collar; 2 denotes the sample; 3 denotes 0.05 mm Pt lead; 4 denotes the boron nitride pressure transmitting medium; 5 denotes the Pb manometer; 6 denotes the Au foil for current leads.

work[12] showed that at superconducting temperatures these materials exist as a mixed $R\bar{3}$ and $P\bar{1}$ phase. In a related study[13] we pointed out the importance of oxygen on the superconducting properties and their pressure dependence for divalent Chevrel phase systems. Oxygen may often be inadvertently introduced into these systems during sample preparation. Previous work showed that an oxygen defect strongly affects T_c at ambient and high pressures in the Chevrel phases.[14]

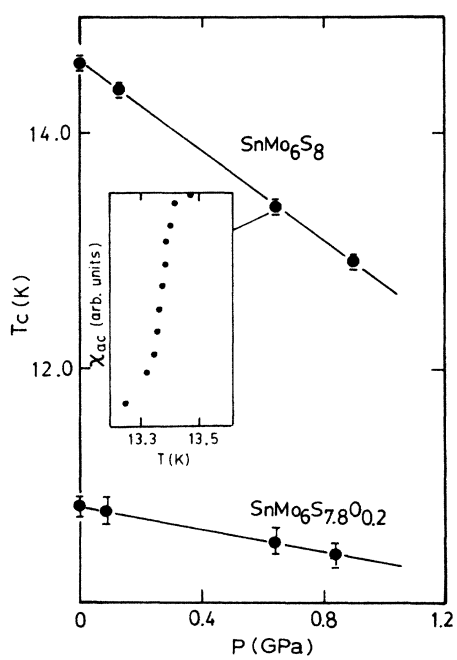

FIG. 2. Superconducting transition temperature vs hydrostatic pressure for a pure and an oxygenated $SnMo_6S_8$ sample, showing the depression of T_c and its pressure dependence with increasing oxygenation. The inset shows the narrow width of T_c, unchanged by increasing pressure. Data are from Ref. 3.

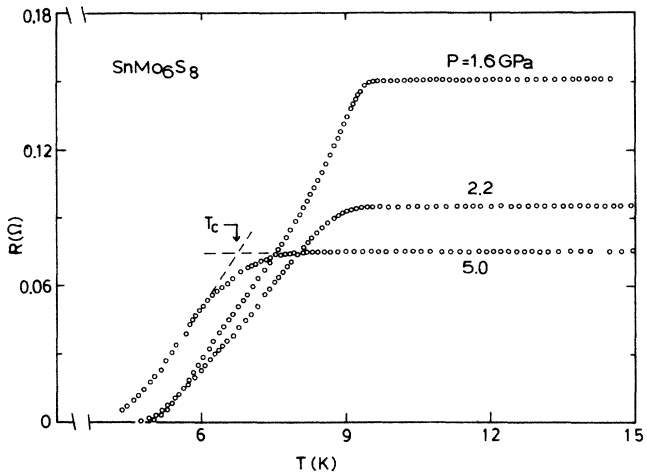

FIG. 3. Quasihydrostatic pressure dependence of the electrical resistance vs temperature for unoxygenated $SnMo_6S_8$. The onset T_c is defined for the 5.0 GPa data.

In this paper, we present comprehensive data on the pressure dependence of the electrical resistivity of three representative divalent Chevrel phase systems: $SnMo_6S_8$, which superconducts at ambient pressure, and $EuMo_6S_8$ and $BaMo_6S_8$, both of which are pressure-induced superconductors. Hydrostatic pressures to 2 GPa were used as well as quasihydrostatic pressures to 10 GPa. Nearly complete T_c versus pressure superconducting normal phase diagrams are presented for all samples studied. For the Sn- and Eu-based systems, the effect of deliberate oxygenation of the samples is shown to suppress T_c as well as its pressure dependence for $P < 3.5$ GPa, but for $P > 3.5$ GPa, the oxygenated and pure samples have similar properties. Several representative electrical resistivity versus temperature data $\rho(T)$ are presented. At very high pressures in the oxygenated $EuMo_6S_8$ system, superconductivity is suppressed and semiconducting electrical resistivity is seen. This feature is seen in the data of Ref. 10 but was not discussed. The data on the $BaMo_6S_8$ sam-

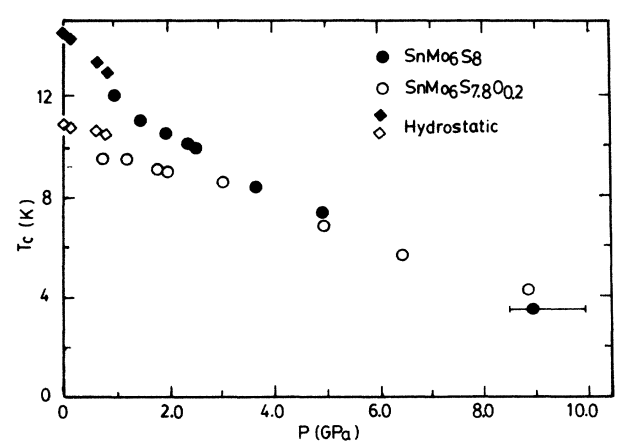

FIG. 4. T_c vs hydrostatic (diamonds) and quasihydrostatic (circles) pressure for a pure and an oxygenated Sn-based Chevrel phase superconductor.

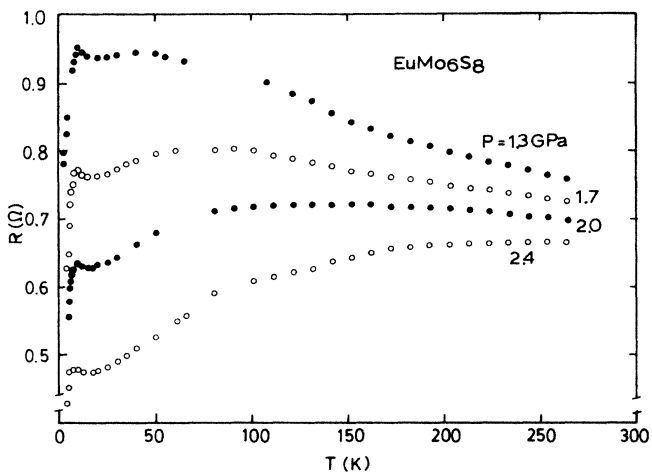

FIG. 5. Resistance vs temperature for a pure $EuMo_6S_8$ sample at various quasihydrostatic pressures. For $P > 2.5$ GPa, metallic resistance is seen over the entire temperature range.

ple are consistent with a pressure-induced transformation to a bulk superconducting state for $P > 2$ GPa. ($EuMo_6S_8$ was previously shown to be fully superconducting for $P > 1.3$ GPa from high-pressure critical field and heat capacity measurements.[14]) Finally, the data from this and other studies are discussed in terms of a model which links the structural transition temperature and T_c for all divalent Chevrel systems. In this model the role of pressure is seen consistently to suppress the structural transition temperature. In the next section we discuss the experimental details used in performing the pressure studies. In the third section, the pressure-related data are presented and discussed, and in the last section, we discuss these data in terms of the model linking T_c, the role of pressure, and the structural transition temperature.

EXPERIMENTAL DETAILS

The samples were prepared by methods previously discussed.[13,15,16] Care was taken to minimize the inadvertant introduction of oxygen into the samples, except in the cases where deliberate oxygen was introduced through controlled addition of MoO. All samples were in the form of polycrystalline sintered lumps. For the hydrostatic measurements, care was also exercised to minimize strains in the samples, because this was shown to broaden the superconducting transition widths.[3] As a result, for these measurements there was no broadening of T_c as pressure increased, and, e.g., T_c (10%–90%) was about 0.1 K for pure $SnMo_6S_8$.

Hydrostatic pressure measurements of T_c were made to about 2 GPa using ac susceptibility at about 16 Hz with the sample in a small self-locking pressure clamp device. The clamp, which was less than 3 cm long, had an outside diameter of about 1.1 cm, and a bore of 1.5 mm.

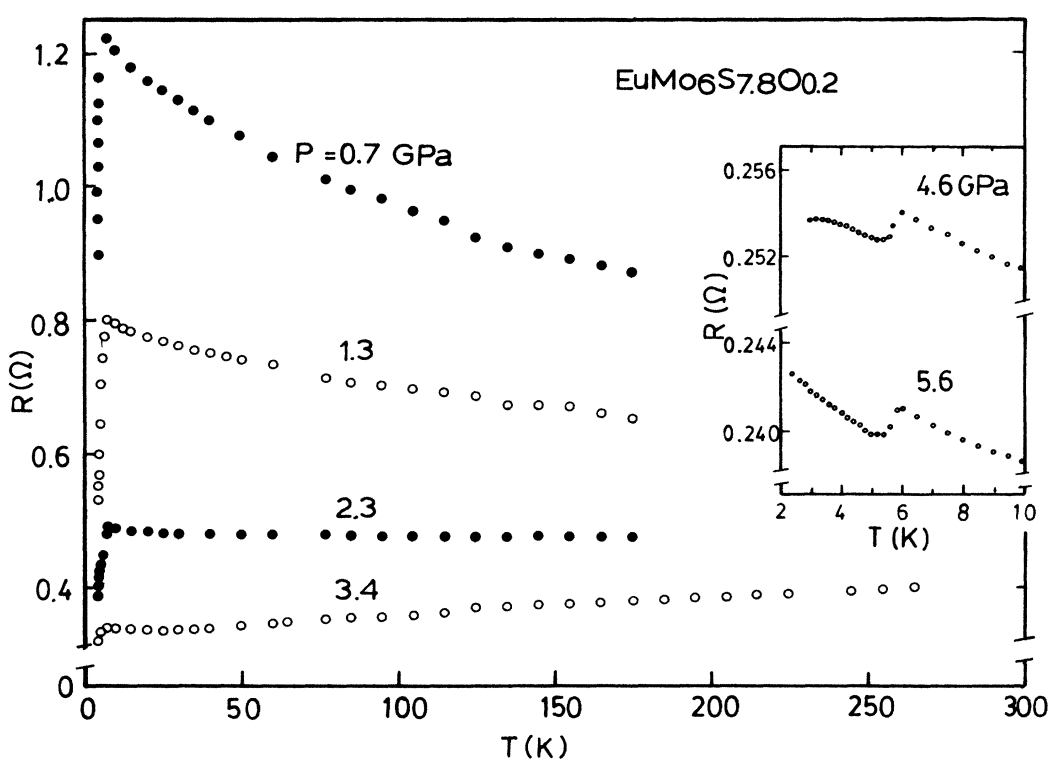

FIG. 6. Resistance vs temperature for an oxygenated Eu-based sample for several quasihydrostatic pressures. The inset shows very high pressure data showing the rise in resistance at lower temperatures at pressures above that needed to suppress superconductivity fully. The small transitions are probably due to pressure inhomogeneities in the cell and represent much less than 1% of the sample resistance.

Small tungsten carbide pistons entered the bore from both ends and were held in place securely by locknuts. A superconducting Pb manometer was used to determine the pressure at low temperatures.

Quasihydrostatic pressures were applied using a self-locking beryllium copper clamp device with opposed tungsten carbide anvils. The overall dimensions of the clamp were length 10 cm, diameter 3 cm, and the working area where pressure was highest between the anvils was about 1 mm^2. The region between the anvils and a top view of the high-pressure region are shown in Fig. 1. A small superconducting Pb manometer was included in the high-pressure region between the anvils as shown. The sample and manometer were imbedded in boron nitride, which acted as a pressure transmitting medium, and this was surrounded by a pyrophilite ring which restricted motion of the pressure medium. Electrical lead access to the samples was by way of 0.05 mm platinum wires fed through microslots in the pyrophilite. The current leads terminated on Au foil contacts. All measurements were made with currents sufficiently weak so as not to perturb the superconducting properties being measured; currents used were typically a few microamperes. The temperature of this clamp was altered by carefully lowering the clamp above a bath of liquid helium. Two separate calibrated thermometers were employed, a silicon diode resistor and a germanium resistance thermometer, both located next to the pressurized sample.

EXPERIMENTAL RESULTS

In Fig. 2 we reproduce results from Ref. 3 showing the pressure dependence of T_c for two $SnMo_6S_8$ samples, one pure and the other with 2.5% O_2 introduced into the S sublattice, making the nominal composition $SnMo_6S_{7.8}O_{0.2}$. Increased oxygenation results in multiphase material. The inset of Fig. 2 shows that the very narrow width of the transition, determined here with ac susceptibility, is not broadened by pressure. Oxygenation clearly decreases T_c, as well as its pressure dependence. In Ref. 3 we demonstrated that three divalent Chevrel phases, $SnMo_6S_8$, $PbMo_6S_8$, and $EuMo_6S_8$, showed a universal behavior, namely that T_c and its pressure dependence scaled, and with the same scale factor for all three systems.

The low-temperature electrical resistance $R(T)$ for the pure $SnMo_6S_8$ sample is shown for pressures in the quasihydrostatic regime in Fig. 3. The normal resistivity decreases with increasing pressure, which may reflect a closer packing of sample grains in this sintered material. The transition widths of the sample measured in the quasihydrostatic regime are fairly large, but this is consistent with the extreme strain dependence of the transition widths noted earlier.[3] However, the onset of T_c, defined in Fig. 3 for the 5.0 GPa data, is not strongly affected by strains,[3] and thus can be used to characterize T_c versus pressure. Figure 4 shows the T_c-P superconducting normal phase diagram for both $SnMo_6S_8$ samples. The hydrostatic and quasihydrostatic data agree fairly well. Also indicated is the pressure gradient in the cell at the highest pressure, determined by the width of T_c of a superconducting Pb manometer. This is extremely narrow at low pressures ($\Delta P < 0.2$ GPa at 2.0 GPa), but broadens nonlinearly with pressure at highest pressures, possibly due to anvil deformation. From Fig. 4 the two phase diagrams are seen to converge for $P > 3.5$ GPa. The extrapolated upper critical pressure P_{c2} for complete suppression of superconductivity is about 12 GPa.

Unlike $SnMo_6S_8$, $EuMo_6S_8$ superconducts only above a critical pressure P_{c1}. At ambient pressure $EuMo_6S_8$ exhibits a rhombohedral-to-triclinic ($R\bar{3}$-to-$P\bar{1}$) structural phase transition which is completed by about 100 K (Ref. 5). Both P_{c1} and the pressure dependence of T_c above P_{c1} depend on oxygen content of the sample.[15] In Fig. 5 we show $R(T)$ for unoxygenated $EuMo_6S_8$ for several pressures. This shows the trend to increasing metallic behavior ($d\rho/dT > 0$) as pressure increases, and above 2.5 GPa

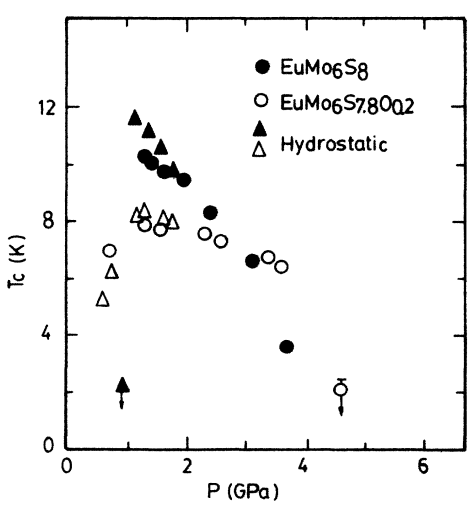

FIG. 7. T_c vs hydrostatic and quasihydrostatic (circles) pressure for a pure and an oxygenated Eu-based Chevrel phase superconductor.

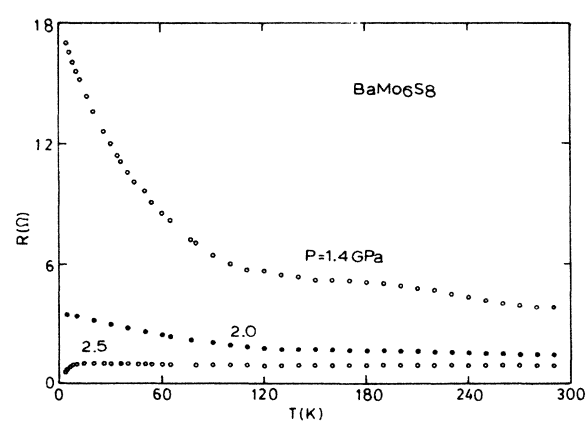

FIG. 8. Resistance vs temperature at three quasihydrostatic pressures for a pure $BaMo_6S_8$ sample. Precursive superconductivity is seen for the $P = 2.5$ GPa data.

metallic conductivity is seen over nearly the entire temperature range studied. For $EuMo_6S_{7.8}O_{0.2}$, $R(T)$ behaves somewhat differently, as can be seen in Fig. 6. Although $d\rho/dT > 0$ for $P > 2.5$ GPa over most of the temperature range, a small increase in $R(T)$ is seen just above the onset of the superconducting transition. This feature, also seen in the "pure" sample, persists to very high pressures and was also observed by Janawadkar *et al.*[10] At pressures above $P_{c2} = 4.5$ GPa, the resistivity increases sharply as temperature decreases, and this is shown in the inset of Fig. 6. The small decrease in $R(T)$ shown in the inset represents less than 1% of the total resistivity, and we suspect this is a highly incomplete transition to superconductivity due to a small portion of the sample located outside the highest pressure region of the clamp. The downturn at 2 K for the 4.6 GPa data is probably the onset of a full superconducting transition. The feature to be stressed here is the indication of semiconducting behavior at pressures well above P_{c2}, which is about 4.5 GPa. This was also observed in Ref. 10. The extent of the upturn in $R(T)$ seems to correlate with oxygen content, increasing (decreasing) with increasing (decreasing) oxygen content.

Figure 7 is a composite of the onset temperatures for T_c versus P for both the pure and oxygenated $EuMo_6S_8$ samples. As noted from the previous study,[15] from which the hydrostatic pressure data in Fig. 7 are derived, P_{c1} is lower for the oxygenated sample. As in the Sn-based study, for $P > 3.5$ GPa, the two phase boundaries tend to merge, although the upper critical pressure is much lower than for $SnMo_6S_8$. The data of Fig. 7 agree fairly well with those of Ref. 10, but the very high pressure upturns in $\rho(T)$ at low temperatures in their data may indicate the presence of some oxygen in their sample.

The high-pressure resistivity studies of Hor *et al.*[7] on $BaMo_6S_8$ pointed to pressure-induced superconductivity, analogous to $EuMo_6S_8$, and partial interface superconductivity was proposed. However, hydrostatic pressures to 1.6 GPa failed to show superconductivity.[8] In Fig. 8 we see a clear indication of the approach to metallic behavior and precursive superconductivity with increasing

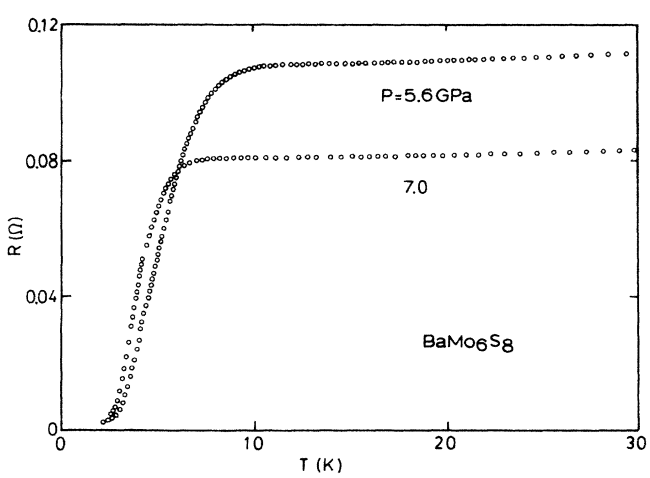

FIG. 9. Full superconducting transitions for $BaMo_6S_8$ at two high quasihydrostatic pressures.

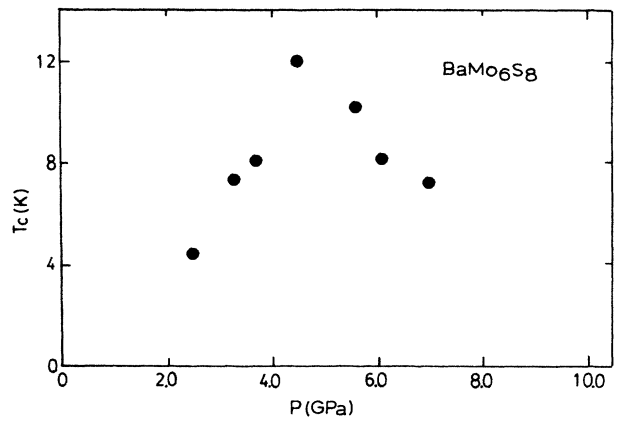

FIG. 10. T_c (onset) vs pressure for $BaMo_6S_8$.

pressure. Figure 9 shows transitions for $BaMo_6S_8$ for two high pressures. (A small zero offset of the measuring apparatus is seen in Fig. 9; the lowest temperature data represent zero resistance.) These transitions are narrower and more convincingly complete than has been previously observed, probably due to the high purity of the sample ("oxygen-free") and because of the relatively narrow range of pressure in these measurements (typically $\Delta P < 0.2$ GPa around 3–5 GPa).

Figure 10 shows the superconductivity onset temperatures versus pressure for $BaMo_6S_8$. As with all the Chevrel systems examined to date, sufficiently high pressure eventually suppresses T_c completely; here above 10 GPa. For $BaMo_6S_8$, P_{c1} is about 4.4 GPa, much larger than that of $EuMo_6S_8$, which probably reflects the higher structural transition temperature (at $P = 0$) in $BaMo_6S_8$. We believe the data presented here indicate a bulk superconducting state for $BaMo_6S_8$, at least for $3 < P < 15$ GPa, in analogy with $EuMo_6S_8$, where high-pressure heat

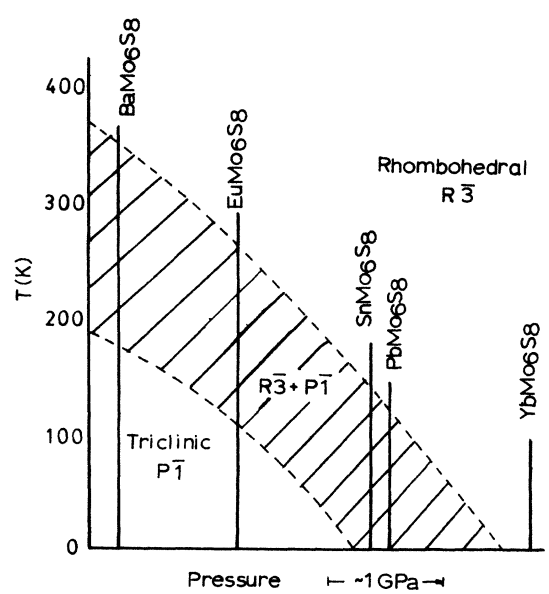

FIG. 11. Schematic illustration of the relationship of the structural transition, the mixed phase region ($R\bar{3}$-$P\bar{1}$), and the role of pressure for divalent Chevrel phases.

capacity and critical field measurements proved that the system is fully superconducting above about 1.3 GPa.[14] Unlike $EuMo_6S_8$, however, where P_{c2} is about 4.5 GPa, T_c for $BaMo_6S_8$ does not decrease rapidly to 0 K, and P_{c2} extrapolates to well above 10 GPa.

DISCUSSION

The data presented above show rather complete superconducting normal phase diagrams for three representative divalent Chevrel phase systems. In addition, the role of oxygen in suppressing P_{c1} and the maximum T_c is detailed in these data. For P immediately above P_{c1} the systems are probably in the mixed $R\bar{3}$-$P\bar{1}$ state, analogous to $SnMo_6S_8$ and $PbMo_6S_8$ at ambient pressure. We note that above about 3.5 GPa the oxygenated and unoxygenated sample phase diagrams merge for the Sn- and Eu-based systems. The role of pressure, the structural transition, and the mixed phase region may be illustrated schematically, as shown in Fig. 11, which is reproduced from Ref. 12. In this plot we show the mixed $R\bar{3}$-$P\bar{1}$ phase regime (shaded) and the position of the various divalent Chevrel systems. The vertical scale is the temperature axis. Pressure is seen to move these positions to the right on Fig. 11. Thus, at helium temperatures it requires about 2 GPa to bring $BaMo_6S_8$ into the mixed phase regime containing the $R\bar{3}$ (superconducting) phase, like the Sn- or Pb-based systems at ambient pressure. Oxygen introduced into the lattice modifies this picture by blurring the position of the phase boundaries of the mixed regime and lowering the T_c that occurs upon entering the superconducting phase.

In this work we have tried to summarize the role of high-pressure on the superconducting transition temperatures of Chevrel phases. The role of oxygen is also examined; oxygen is often inadvertantly introduced into the lattice and is a likely constituent in any large scale use of Chevrel phases for technological applications. The data are consistent with a schematic plot showing the interplay of the $R\bar{3}$-$P\bar{1}$ structural transition, high pressure, and the existence of superconductivity.

ACKNOWLEDGMENTS

We are pleased to acknowledge encouragement and helpful discussions with Dr. Simon Foner of the Francis Bitter National Magnet Laboratory, M.I.T., where most of the experimental work presented in this paper took place. This work was supported by the National Science Foundation under Grant No. DMR 85-02077. The work at Argonne National Laboratory was supported by the U.S. Department of Energy, DOE/BES W-31-109-ENG-38.

[1]For an extensive review, see *Superconductivity in Ternary Compounds I,* Vol. 32 of *Topics in Current Physics,* edited by O. Fischer and M. B. Maple (Springer-Verlag, New York, 1982), and *Superconductivity in Ternary Compounds II,* Vol. 34 of *Topics in Current Physics,* edited by M. B. Maple and O. Fischer (Springer-Verlag, New York, 1982). See also the review of O. Fischer, Appl. Phys. **16**, 1 (1978).

[2]H. W. Meul, C. Rossel, M. Decroux, O. Fischer, G. Remenyi, and A. Briggs, Phys. Rev. Lett. **53**, 497 (1984).

[3]D. W. Capone II, R. P. Guertin, S. Foner, D. G. Hinks, and H. C. Li, Phys. Rev. B **29**, 6375 (1984).

[4]C. Rossel, H. W. Meul, A. Junod, R. Baillif, O. Fischer, and M. Decroux, Solid State Commun. **48**, 431 (1983).

[5]R. Baillif, A. Dunand, J. Muller, and K. Yvon, Phys. Rev. Lett. **47**, 672 (1981).

[6]C. W. Chu, S. F. Huang, C. H. Lin, R. L. Meng, M. K. Wu, and P. H. Schmidt, Phys. Rev. Lett. **46**, 276 (1981); D. W. Harrison, K. C. Lim, J. D. Thompson, C. Y. Huang, P. D. Hambourger, and H. L. Luo, *ibid.* **46**, 280 (1981).

[7]P. H. Hor, M. K. Wu, T. H. Lin, X. Y. Shao, X. C. Jin, and C. W. Chu, Solid State Commun. **44**, 1605 (1982); W. A. Kalsbach, R. W. McCallum, V. Poppe, F. Pobell, R. N. Shelton, and P. Klavins, in Proceedings of the International Conference on Superconductivity in *d*- and *f*-Band Metals, edited by W. Buckel and W. Weber, Karlsruhe, 1982 (unpublished), p. 185.

[8]C. Rossel, M. Decroux, and O. Fischer, in *LT-17,* edited by U. Eckern, A. Schmidt, W. Weber, and H. Wuhl (Elsevier, New York, 1984), pp. 337 and 338.

[9]R. N. Shelton, in *Superconductivity in d- and f-Band Metals,* Proceedings of the 2nd Rochester Conference, edited by D. H. Douglass (Plenum, New York, 1976), pp. 137–159.

[10]M. P. Janawadkar, V. Sankara Sastry, Y. Hariharan, and T. S. Radhakrishnan, J. Low Temp. Phys. **54**, 411 (1984).

[11]J. D. Jorgensen and D. G. Hinks, Solid State Commun. **53**, 289 (1985).

[12]J. D. Jorgensen, D. G. Hinks, and G. P. Felcher, Phys. Rev. B **35**, 5365 (1987).

[13]D. G. Hinks, J. D. Jorgensen, and H.-C. Li, Solid State Commun. **49**, 51 (1984).

[14]M. Decroux, S. E. Lambert, M. S. Torikachvili, M. B. Maple, R. P. Guertin, L. D. Woolf, and R. Baillif, Phys. Rev. Lett. **52**, 1563 (1984).

[15]D. W. Capone, R. P. Guertin, S. Foner, D. G. Hinks, and H.-C. Li, Phys. Rev. Lett. **51**, 601 (1983).

[16]D. G. Hinks, J. Jorgensen, and H.-C. Li, Phys. Rev. Lett. **51**, 1911 (1983).